International Journal of Innovative Science and Modern Engineering (IJISME)
ISSN: 2319-6386 (Online), Volume-12 Issue-11, November 2024

Heat and Mass Transfer in Unsteady MHD Casson Fluid Flow Over a Semi-Infinite Vertical Plate Through Porous Medium with Dissipative and Radiative Effects

Muhammad Minarul Islam, Riaz Hossain

Abstract: Nowadays, Casson fluid and its diverse applications are highly effective across a vast array of industrial, biological and environmental sectors, due to its unique flow properties. This study focuses on the numerical investigation of the heat and mass transfer characteristics of an unsteady incompressible Casson fluid flow over a semi-infinite vertical flat plate by considering free convection effects. The fluid is conducting the electrical current as it moves through the porous medium. The formulation of the governing equation is based on the use of this phenomenon. In the model, the formulated governing equations are converted into non-dimensional form first, and the MHD mathematical model is analyzed using the boundary conditions. The scheme of finite difference method is implemented to solve the model, where concentration profiles are also discussed. Stability and convergence criteria are applied for the accuracy of numerical techniques, and the effects of various parameters on skin friction, rate of heat and mass transfer have been examined significantly. The results indicate that the temperature of the plate increases with the increase in the value of the magnetic parameter for the Casson fluid but the reverse is observed in its limiting case. The present results are compared and checked with previously published results and a remarkable conclusion is given at the end of the study.

Keywords: Casson Fluid, Chemical Reaction, Heat and Mass Transfer, MHD, Porous Media, Semi-Infinite Plate, Thermal Radiation.

I. INTRODUCTION

Fluid dynamics is a charming branch of science that explores the complicated patterns and actions of liquids and gases as they flow and interact with their surroundings. It's a mesmerizing trip that unravels the riddle of motion from the gentle ripples of a sluice to the powerful currents of an ocean and the nimble flight of an aeroplane through the sky.

Manuscript received on 30 November 2024 | Revised Manuscript received on 26 October 2024 | Manuscript Accepted on 15 November 2024 | Manuscript published on 30 November 2024.
*Correspondence Author(s)
Dr. Muhammad Minarul Islam, Department of Mathematics, Bangabandhu Sheikh Mujibur Rahman Science and Technology University, Gopalganj, Dhaka, Bangladesh Email ID: minarul_math@bsmrstu.edu.bd
Riaz Hossain*, Department of Mathematics, Bangabandhu Sheikh Mujibur Rahman Science and Technology University, Gopalganj, Dhaka, Bangladesh Email ID: riaz.17mat069@bsmrstu.edu.bd, ORCID ID: 0009-0005-6611-7687

In the field of fluid dynamics, there exists a classification system that encompasses two distinct orders of liquids, specifically Newtonian andnon-Newtonian fluids. Newtonian fluids are linearly proportional to the stress-strain relationship, and they're unfit to requite for the various properties observed for fluids in industrial and technological applications like as blood, soaps, certain lubricants, paints, pharmaceutical formulations, and numerous emulsions [1]. On the other phase,non-Newtonian fluids have a complicated relationship between shear stress and shear strain and can explain the complex phenomena observed in industrial and technological operations [2]. This is more realistic to model, as numerous real- world fluids arenon-Newtonian. It makesnon-Newtonian fluids a useful instrument for engineers designing any system and for scientists studying the actions of fluids. It is also helpful in predicting interpretation of accoutrements in industrial processes. Casson fluids are notable for their exceptional rheological properties among non-Newtonian fluids and are ideal for studying fluid flow phenomena in various environments. Casson fluids have acquired these non-Newtonian rheological properties due to the shear stress and strain relationship [3]. This fluid exhibits significant shear viscosity and yield stress, making it an excellent choice for shear- thinning applications [4].

Casson fluid is a shear-thinning liquid that has infinite viscosity at a zero rate of shear, yield stress below which no flow occurs, and a zero viscosity at an infinite rate of shear [5]. In simpler words, for Casson fluid to flow, it must overcome the yield shear stress; otherwise, the fluid behaves as a solid. Some of the most common Casson fluids include jelly, tomato sauce, honey, concentrated fruit juices, paint, and drilling fluids. Even human blood is regarded as Casson fluid [6]. The plasma in human red blood cells contains various components, including proteins, fibrinogen, and globulin, which can combine into chain-like structures known as aggregates or rouleaux [7]. This arrangement aligns with the principles of Casson fluid theory, suggesting that blood flows more smoothly when it experiences low shear rates and is travelling through small blood vessels. Casson fluids are found to be applicable in developing models for blood oxygenators, hemodialyzers, and cardiovascular systems.

The application of Casson fluids has been growing rapidly, and as a result, many researchers are concentrating on their characteristics.

*Published By:
Blue Eyes Intelligence Engineering and Sciences Publication (BEIESP)*

If the rouleaux display plastic-solid behavior, the yield stress can be identified with the continuous yield stress in Casson fluid, as investigated by Fung et al [8]. Mustafa et al [9]. studied the unsteady flow and heat transfer of a Casson fluid past a moving flat plate using the homotopic technique. Deepa et al [10]. studied stratified Casson fluid flows with generative or destructive heat energy, solving the problem using the implicit finite difference method. Sharidan Shafie et al [11]. explored MHD free-convection Casson fluid flow over oscillating vertical plates using similarity transformations and bvp4c.

Magneto-hydrodynamics (MHD) is a branch of plasma physics and continuum mechanics that studies the behavior of electrically conducting fluids under electromagnetic forces. It has gained significant attention due to its relevance to astrological and geophysical phenomena and its applications in various industries, including industrial, mechanical, civil, chemical, and biomechanical processes. MHD flows can be complex when accompanied by non-Newtonian fluids like Casson fluids and porous media. Accurate numerical simulations of MHD flows with non-Newtonian fluids are crucial for predicting and optimizing industrial operations. Various studies have investigated the behavior of these complex flows to understand and control the effects of the magneto-hydrodynamic force. Khalid et al [12]. solved the transient flow of Casson fluid over a vertical oscillatory plate embedded in a porous medium using the Laplace transform method. Siva Raj et al [13]. studied MHD Casson fluid flow over a vertical cone and flat plate with non-uniform heat source/sink effects using the Crank-Nicolson finite difference scheme. M.C. Raju et al [14]. investigated unsteady MHD natural convective Casson fluid flow towards a vertical plate with an angle of inclination using the finite element method. Poornima et al [15]. explored the unsteady magneto hydrodynamic flow of non-Newtonian fluid through a vertical plate in the presence of Hall current.

Industrial processes involve heat and mass transfer, leading to a flow field influenced by density differences, concentration gradients, and material composition. Two major effects are the diffusion-thermo effect (Dufour effect) and the thermal-diffusion effect (Soret effect). These effects are often overlooked in heat and mass transfer analysis, but they can be significant under specific conditions, especially in petrology, geosciences, chemical engineering, thermal and insulating engineering, and modeling of packed sphere beds. Researchers can achieve more accurate and realistic results in industrial processes and energy systems by incorporating Dufour and Soret effects [16]-[18].

Radiative-convective flow phenomena are crucial in various industrial and environmental systems, including space technology and high-temperature research [19]. These flows have led to extensive investigations into the interplay between free convection and heat radiation in hydrodynamic and magneto-hydrodynamic scenarios, considering various physical and geological factors. Thermal radiation effects have been suggested to play a significant role in controlling heat transfer during polymer processing [20], while thermal radiation is included in the temperature field equation [21].

A semi-infinite plate is a planar surface that extends infinitely in one direction but not in the other. In fluid dynamics, a semi-infinite vertical flat plate is oriented vertically and has dimensions that are infinite in the vertical direction but limited in the horizontal direction. When a fluid flows over a semi-infinite vertical flat plate, it generates a boundary layer with significant fluid velocity and temperature gradients. This boundary layer evolution is crucial for heat and mass transfer characteristics in industrial processes like chilling systems, aerodynamics, and chemical engineering [21]. Amanulla et al [22]. studied the transfer of natural convective nanofluid flow past a vertical plate surface, focusing on velocity and thermal slip effects and found that nanoparticle concentrations decrease with increased slip parameters, potentially impacting electric-conductive nanomaterials in aerospace and other industries. Deekshitulu et al [23] [24]. explored radiation absorption in unsteady MHD free convection Casson fluid flow.

This study is a significant advancement in the field of Casson fluid flow, focusing on the steady-state solution of unsteady Casson fluid flow. The model is represented by a system of partial differential equations (PDEs), simplified using conventional transformations. The finite difference method is used to obtain the numerical solution for this innovative retrieval system. The main objective is to verify the accuracy of the numerical technique by conducting stability and convergence evaluations. The study explores the effects of key parameters on variables such as skin fraction, heat transfer rate, and mass transfer, as well as their influence on velocity, temperature, and concentration. The impacts are comprehensively examined and clearly depicted through graphical illustrations. Comparison analyzes with previous studies by Sandeep et al [25]., K. K. Asogwa et al. [26], and M. Das et al [1]. are conducted to provide context and contribute to the current body of knowledge. The research concludes with a concise deduction that succinctly synthesizes its principal findings and implications. The frameworks are as follows: Section II explains the model under consideration with its mathematical representation. Section III represents numerical approaches for solving the model. Convergence and stability criteria are discussed in Section IV and engineering curiosity (shear stress, Nusselt and Sherwood number) is addressed in Section V. The result and discussion are represented in Section VI. In Section VII, the concluding remarks are provided.

II. MODEL ESTABILISHMENT AND ANALYSIS

Consider an unsteady incompressible fluid in electrically conducting, thermally radiating and dissipative Casson fluid flow past a semi-infinite vertical flat plate at $y'=0$ through the porous medium. The fluid flow assumed to be in the x' direction which is chosen along the plate in upward direction and y' axis is the normal to the plate as shown in Fig.1. A uniform magnetic field is applied parallel to the y' axis. At time $t' \leq 0$, the plate and fluid are at same with the ambient temperature. At time $t' > 0$, the plate starts exponentially accelerated with the velocity $U_0 e^{at'}$ in its own plane and the plate temperature and concentration is raised to

Published By:
Blue Eyes Intelligence Engineering
and Sciences Publication (BEIESP)

$T'_\infty + (T'_W - T'_\infty)\frac{t'}{t_0}$ and $C'_\infty + (C'_w - C'_\infty)\frac{t'}{t_0}$ respectively, and thereafter T'_w and C'_w i.e. at $t' > t_0$, plate maintained at uniform temperature and concentration.

Since the plate extends infinitely in the x-direction and has a finite extent in another direction, all physical parameters, with the exception of pressure, are

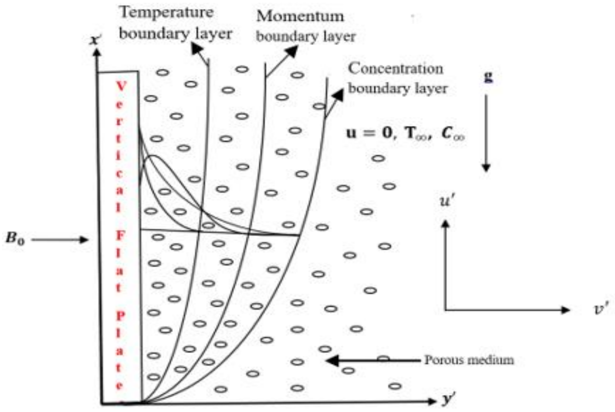

[Fig. 1: Physical Problem and co-Ordinate System]

exclusively functions of the vertical coordinate y' and t'. Also assume that, the radiative heat flux q_r is applied in the normal to the plate and the magnetic Reynolds number of the flow is small enough so that the Induced magnetic field is negligible. By the Roseland approximation radiative heat flux is given by $q_r = -\frac{\sigma *}{3k*}\nabla T$,where σ^* and k^* are Stefan Boltzmann comfort and the Roseland mean absorption coefficient respectively. We assume that are sufficiently small such that T^4 may be expressed a linear function of temperature i.e. $T^4 = 4T_\infty^3 - 3T_\infty^4$. Then, the radiative heat flux can be written as,

$$q_r = -\frac{\sigma^* 4T_\infty^3}{3k^*}\frac{\partial^2 T'}{\partial y'^2}$$

The rheological equation governing the behavior of an isotropic and incompressible material. The Casson fluid can be expressed in the following manner.

$$\tau = \begin{cases} 2\left(\mu_b + \frac{\tau_0}{\sqrt{2\pi_c}}\right)e_{ij}\pi_c > \pi \\ 2\left(\mu_b + \frac{\tau_0}{\sqrt{2\pi_c}}\right)e_{ij}\pi_c < \pi \end{cases}$$

where, τ_0 is known as the yield stress of the fluid, mathematically expressed as,

$$\tau_0 = \frac{\mu_b\sqrt{2\pi}}{\eta}$$

here, the symbol π denotes the multiplication of the deformation rate with itself $\pi = e_{ij}.e_{ij}$, where e_{ij} represents $(i, j)th$ element of measure of deformation and π_c is the critical value based on the non-Newtonian model. In the case of Casson fluid flow where $\pi > \pi_c$ .So it is possible to say that, $\mu = \mu_b\left(1+\frac{1}{\eta}\right)$

where, μ_b is the plastic dynamic viscosity of Casson fluid and η is the Casson parameter.

As η increases, it has a notable effect on the viscosity of the Casson fluid. Specifically, as η increases, the viscosity of the Casson fluid decreases. This phenomenon is particularly intriguing because, as η approaches infinity, the Casson fluid behaves in a manner akin to that of a Newtonian fluid. In essence, the Casson fluid transitions towards a Newtonian-like behavior when η becomes extremely large. This transformation in behavior signifies the intriguing and important rheological properties of Casson fluids, where the Casson parameter plays a pivotal role in determining the fluid's viscosity characteristics.

Since Casson fluid through the porous medium, so Darcy law is applicable to it. Dary law can be define as,

$$R = -\frac{\mu_b}{k}\left(1+\frac{1}{\eta}\right)q_d$$

For porous medium, the intrinsic velocity is used to balance the Darcy velocity with the help of Dupuit-Forchheeimer relationship $q_d = \varphi q$,then modified darcy law can be express as,

$$R = -\frac{\mu_b}{k}\left(1+\frac{1}{\eta}\right)\varphi q$$

From the above assumption, the system of coupled non-linear partial differential equations under the competent boundary layer equation are given as follows:

A. Momentum Equation

$$\left\{\begin{array}{l}\frac{\partial u'}{\partial t'} = g\beta(T'-T'_\infty) + g\beta^*(C'-C'_\infty) \\ +\frac{\mu_b}{\rho}\left(1+\frac{1}{\eta}\right)\frac{\partial^2 u'}{\partial y'^2} - \frac{\mu_b\varphi}{\rho k_1}\left(1+\frac{1}{\eta}\right)u' - \frac{\sigma B_0^2 u'}{\rho}\end{array}\right\} \quad (1)$$

B. Energy Equation

$$\left\{\begin{array}{l}\frac{\partial T'}{\partial t'} = \frac{k}{\rho c_p}\frac{\partial^2 T'}{\partial y'^2} + g\beta^*(C'-C'_\infty) \\ +\frac{\mu_b}{\rho c_p}\left(1+\frac{1}{\eta}\right)\left(\frac{\partial u'}{\partial y'}\right)^2 + \frac{16}{\rho c_p}\frac{\sigma^* 4T_\infty^3}{3k^*}\frac{\partial^2 T'}{\partial y'^2} \\ -\frac{Q_1}{\rho c_p}(T'-T'_\infty) + \frac{D_m K_T}{c_p c_s}\frac{\partial^2 C'}{\partial y'^2} + \frac{\sigma B_0^2 u'^2}{\rho c_p}\end{array}\right\} \quad (2)$$

C. Concentration Equation

$$\left\{\frac{\partial C'}{\partial t'} = D_m\frac{\partial^2 C'}{\partial y'^2} - K_r(C'-C'_\infty) + \frac{D_m K_T}{T_m}\frac{\partial^2 T'}{\partial y'^2}\right\} \quad (3)$$

The boundary settings for the governing system of non-linear partial differential equations are specified as follows, (see on [21])

$$t' \le 0 : u' = 0, T' = T_\infty, C' = C_\infty everywhere$$

Published By:
Blue Eyes Intelligence Engineering
and Sciences Publication (BEIESP)

$$\left.\begin{array}{l} t'>0: u'=U_0 e^{\alpha' t'} \\ 0<t'<t_0: T'=T_\infty+(T_w'-T_\infty')\dfrac{t'}{t_0} \\ C'=C_\infty+(C_w'-C_\infty')\dfrac{t'}{t_0} \\ t'>t_0: T'=T_w', C'=C_w' \end{array}\right\} \text{ at } y'=0 \qquad (4)$$

$$u'\to 0, T'\to T_\infty, C'\to C_\infty \text{ at } y'\to\infty$$

The utilization of the following dimensionless quantities is employed for the implementation of dimensionless techniques:

$$u=\frac{u'}{U_0}, y=\frac{U_0 y'}{\vartheta}, t=\frac{U_0^2 t'}{\vartheta}, T=\frac{T'-T_\infty'}{T_W'-T_\infty'}$$
$$C=\frac{C'-C_\infty'}{C_W'-C_\infty'}, \alpha=\frac{\vartheta\alpha'}{U_0^2}, t_1=\frac{U_0^2 t_0}{\vartheta}$$

Using the preceding nondimensional assumptions, the governing equations (1) to (4) can be reformulated as nonlinear partial differential equations, as demonstrated by the subsequent equations:

$$\left\{\begin{array}{c}\dfrac{\partial u}{\partial t}=G_r\cdot T+G_m\cdot C+\left(1+\dfrac{1}{\eta}\right)\dfrac{\partial^2 u}{\partial y^2} \\ -\left(1+\dfrac{1}{\eta}\right)\dfrac{u}{K_p}-M\cdot u\end{array}\right\} \qquad (5)$$

$$\left\{\begin{array}{c}\dfrac{\partial T}{\partial t}=\dfrac{1}{P_r}(1+R_a)\dfrac{\partial^2 T}{\partial y^2}+E_c\left(1+\dfrac{1}{\eta}\right)\left(\dfrac{\partial u}{\partial y}\right)^2 \\ -Q\cdot T+D_u\dfrac{\partial^2 c}{\partial y^2}+M\cdot E_c\cdot u^2\end{array}\right\} \qquad (6)$$

$$\left\{\frac{\partial C}{\partial t}=\frac{1}{S_c}\frac{\partial^2 C}{\partial y^2}-K_r C+S_o\frac{\partial^2 T}{\partial y^2}\right\} \qquad (7)$$

The requisite settings for dimensionless initial and boundary conditions are,

$$t\le 0: u=0, T=0, C=0 \text{ everywhere}$$

$$\left.\begin{array}{l} t'>0: u=e^{\alpha t} \\ 0<t<t_1: T=\dfrac{t}{t_1}, C=\dfrac{t}{t_1} \\ t>t_1: T=T_w, C=C_w \end{array}\right\} \qquad (8)$$

$$u\to 0, T\to T_\infty, C\to C_\infty$$

where, $R_a=\dfrac{16\sigma^*}{k^* k}T_\infty^3$ (Radiation parameter),

$E_c=\dfrac{U_0^2}{c_p(T_w-T_\infty)}$ (Eckert number),

$D_u=\dfrac{D_m K_T(C_w-C_\infty)}{c_p c_s \upsilon(T_w-T_\infty)}$ (Dufour number),

$G_r=\dfrac{\vartheta g\beta\ (T_w-T_\infty)}{U_0^3}$ (Thermal grashof number),

$G_m=\dfrac{\vartheta g\beta^*(C_w-C_\infty)}{U_0^3}$ (Solutal grashof number),

$K_p=\dfrac{k_1 U_0^2}{\vartheta^2\varepsilon}$ (Porous permeability parameter),

$S_c=\dfrac{\vartheta}{D_M}$ (Schimdt number),

$K_r=\dfrac{k_r\vartheta}{\upsilon^2}$ (Chemical reaction parameter),

$P_r=\dfrac{\rho c_p\vartheta}{k}$ (Prandtl number),

$S_o=\dfrac{D_m K_T(T_w-T_\infty)}{T_m\upsilon(C_w-C_\infty)}$ (Soret number) and

$Q=\dfrac{D_1\upsilon}{\rho c_p U_0^2}$ (Heat absorption parameter),

$M=\dfrac{\sigma_0\beta_0^2\vartheta}{\rho U_0^2}$ (Magnetic parameter)

III. NUEMERICAL TECHNIQUES

This section concisely presents an overview of the application of the explicit finite difference method (FDM) for solving the regulatory equations (5)-(8).

The fluid flow domain undergoes discretization through the establishment of a grid-oriented perpendicular to the y-direction. This approach enables the concurrent discretization of finite difference equations across temporal and spatial dimensions. In the context of the boundary layer flow region, first-order derivatives are estimated through backward differencing, while higher-order derivatives employ central differencing. Streamlining calculations, an arbitrary assumption situates the free stream region at $y_{\max}=10$, effectively designating it as the $y\to\infty$ region representing the domain of free stream. Following experimentation involving diverse mesh configurations, a grid size of $m=400$ is selected for numerical simulations' execution.

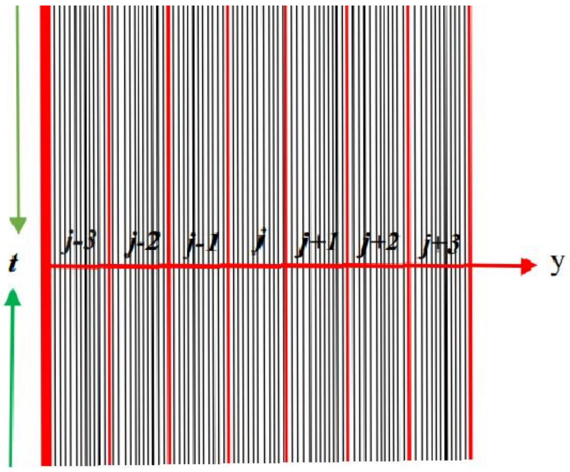

[Fig.2: Finite Difference Scheme]

The configuration of this mesh is visually depicted in Figure 2. In order to ensure consistency, a minor time increment of $\Delta t = 0.0001$ is utilized, while maintaining a uniform mesh size of $\Delta y = 0.025$ in the y direction for the range of $0 < y < 10$. The desired values of u^*, T^* and C^* correspond to the corresponding values of u, T and C at the last time-step. Through the utilization of the explicit Finite Difference Method (FDM) technique, a comprehensive set of discretized equations is methodically constructed, as expounded below,

$$\left\{\begin{array}{l} \frac{u_j^* - u_j}{\Delta t} = G_r.T_j + G_m.C_j \\ +\left(1+\frac{1}{\eta}\right)\frac{u_{j+1} - 2u_j + u_{j-1}}{(\Delta y)^2} - \left(1+\frac{1}{\eta}\right)\frac{u_j}{K} - M.u_j \end{array}\right\} \quad (9)$$

$$\left\{\begin{array}{l} \frac{T_j^* - T_j}{\Delta t} = \frac{(1+R_a)}{P_r}\frac{T_{j+1} - 2T_j + T_{j-1}}{(\Delta y)^2} \\ +E_c\left(\frac{u_j - u_{j-1}}{\Delta y}\right)^2 + D_u\frac{C_{j+1} - 2C_j + C_{j-1}}{(\Delta y)^2} + M.E_c.u_j^2 \end{array}\right\} \quad (10)$$

$$\left\{\begin{array}{l} \frac{C_j^* - C_j}{\Delta t} = \frac{1}{S_c}\frac{C_{j+1} - 2C_j + C_{j-1}}{(\Delta y)^2} - K_r.C_j + \\ S_o\frac{T_{j+1} - 2T_j + T_{j-1}}{(\Delta y)^2} \end{array}\right\} \quad (11)$$

The finite difference method (FDM) schemes are responsible for generating the initial and boundary settings as,

$$t \le 0 : u_j^k = 0, T_j^k = 0, C_j^k = 0 everywhere$$

$$\left.\begin{array}{l} t > 0 : u_0^k = e^{\alpha t} \\ 0 < t < t_1 : T_0^k = k, C_0^k = k \\ t > t_1 : T_0^k = 1, C_0^k = k \end{array}\right\} \quad (12)$$

$$u_{j\_max}^k = 0, T_{j\_max}^k = 0, C_{j\_max}^k = 0$$

The subscript notation j represents the nodal points along the y coordinate, indicating the spatial positions within the computational mesh. On the other hand, the subscript notation k signifies the time iteration step, with time t equal to k multiplied by the time step Δt. Here, k is an integer value ranging from 0 to infinity, representing successive time intervals in the simulation.

IV. QUANTITIES OF ENGINEERING CURIOSITY

This section deals with the entities that have been referred to as having significant relevance to various engineering purpose. It mentions Nusselt number, shear stress and Sherwood number, and their significance in engineering analysis. Shear stress refers to the forces acting parallel to a surface due to the viscous effects of a fluid. In this context, it's related to the landmarks or characteristics of the fluid layer that surrounds a solid plate or surface. The shear stress is expressed as, $\tau = -\left(1+\frac{1}{\eta}\right)\left(\frac{\partial u}{\partial y}\right)_{y=0}$. The Sherwood number is used to determine convection mass transfer efficiency, quantifying the rate at which a substance is transferred from a solid surface into a fluid due to convection. The dimensionless Sherwood number is defined as, $S_h = -\left(\frac{\partial C}{\partial y}\right)_{y=0}$. And, the Nusselt number is used for heat transfer analysis, quantifying the heat transfer efficacy from a solid surface to a fluid. It's dimensionless form is $N_u = -\left(\frac{\partial T}{\partial y}\right)_{y=0}$ .These entities are crucial in understanding the behavior of materials and systems in various engineering applications.

V. CONVERGENCE AND STABILITY ANALYSIS

The stability and convergence of solutions in the explicit finite difference method (FDM) are ensured by the implementation of stability and convergence criteria. By utilizing the stated stability criteria, the steady-state profiles are derived and a more refined mesh configuration is identified. Currently, the stability requirements for discretized equations can be precisely defined as:

$$1+\left(1+\frac{1}{\eta}\right)(\cos\beta\Delta y - 1)\frac{2\Delta x}{(\Delta y)^2} - \left(1+\frac{1}{\eta}\right)\frac{1}{k}\Delta t - M\Delta t \le -1$$

$$1+\frac{(1+R_a)}{P_r}(\cos\beta\Delta y - 1)\frac{2\Delta x}{(\Delta y)^2} - Q\Delta t \le -1$$

$$1+\frac{1}{S_c}(\cos\beta\Delta y - 1)\frac{2\Delta x}{(\Delta y)^2} - K_r\Delta t \le -1$$

When $\Delta t = 0.0001$ and Δy approaches to zero, then the problem will be converged. With the initial boundary conditions are set with the values of $\Delta t = 0.0001$ and $\Delta y = 0.025$, the problem will exhibit convergence at $P_r \ge 0.32$, $R_a \le 1.9$, $K_r \le 20$, $0.32 \le S_c \le 15$, $\eta \ge 0.2$.

VI. RESULT ANALYSIS AND DISCUSSION

In the pursuit of understanding the flow scheme's physical insights, the analysis revolves around several essential parameters that influence various aspects of the system. These parameters encompass the Magnetic parameter (M), Chemical reaction parameter (K_r), Dufour number (D_u), Eckert number (E_c), Casson fluid parameter (η), Porous permeability parameter (K), Schmidt number (S_c), Soret number (S_o), Radiation parameter (R_a),

Published By:
Blue Eyes Intelligence Engineering
and Sciences Publication (BEIESP)

Thermal grashof number $\left(G_r\right)$, Prandtl number $\left(P_r\right)$ and Solutal grashof number $\left(G_m\right)$. The influence of these parameters on velocity, concentration, temperature profiles, local shear stress, Nusselt number and Sherwood number has been graphed and tabulated in the study. The analyses are conducted with a common assumption, wherein values remain fixed at $G_r = 10$, $G_m = 5$, $K_r = 1.0$, $P_r = 0.71$, $S_c = K = 0.6$, $S_o = D_u = Q = R_a = \eta = t_1 = 0.5$, $E_c = 0.05$, $M = 3.0$ and $\alpha = 0.4$, at a steady-state time point $t = 6.0$. The homogeneity of these values is evaluated in the respective figures within the scope of the current investigation.

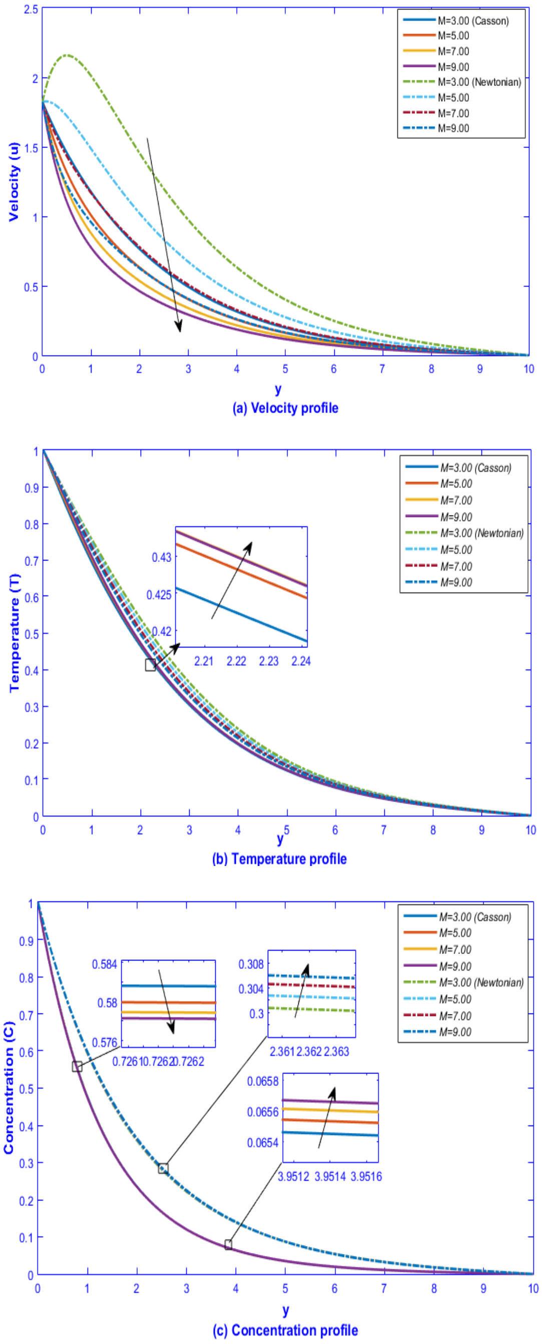

[Fig.3: Influence of Various Values of Magnetic Parameter (M)]

The impact of magnetic parameter on fluid behavior is clearly demonstrated in Figure 6. The velocity reaches its maximum value at the surface of the flat plate, after which it gradually drops as the distance from the plate increases, eventually approaching zero asymptotically. As the magnetic parameter increases, the reducing effect of velocity profiles has been exhibited. The augmentation of magnetic parameters leads to an escalation in the generated Lorentz force inside the boundary layer, consequently resulting in a reduction of the velocity profiles within the noted boundary layer. This observation suggests that an elevation in the magnetic parameter leads to a corresponding rise in the Lorentz force. As a result, the enhanced Lorentz force acts in opposition to the fluid flow, reducing the overall fluid velocity, which is illustrated in Figure 6-a.

A commonly observed requirement in the field of fluid dynamics is that the velocity of a fluid diminishes as the temperature gets higher. A similar result has been dominant in the current investigation, which is expressed in Figure 6-b. It is shown that higher values of the magnetic parameter lead to a reduction in velocity and induce temperature profiles. The decrease in momentum in the boundary layer induces molecular diffusion in the boundary layer. As a result, concentration increases with the increases in the magnetic parameter that have been delineated in Figure 6-c.

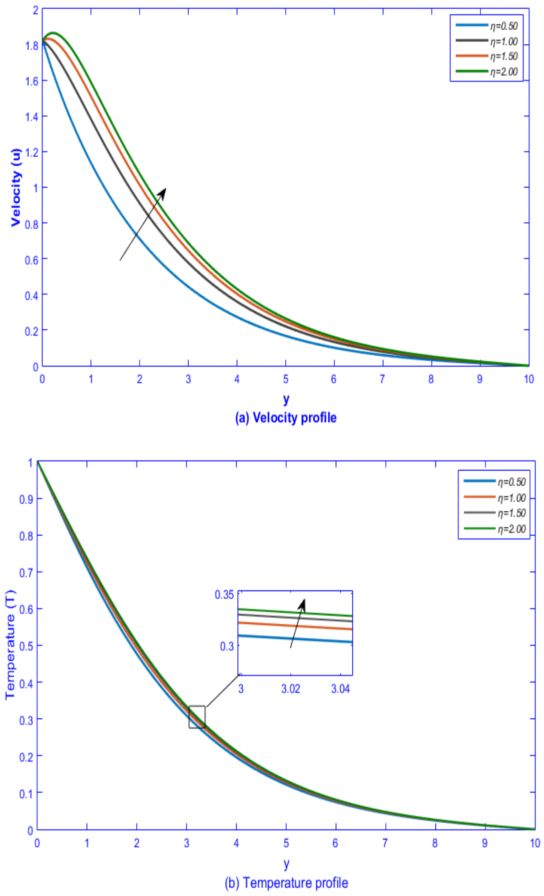

Retrieval Number: 100.1/ijisme.E79740112524
DOI: 10.35940/ijisme.E7974.12111124
Journal Website: www.ijisme.org

Published By:
Blue Eyes Intelligence Engineering
and Sciences Publication (BEIESP)

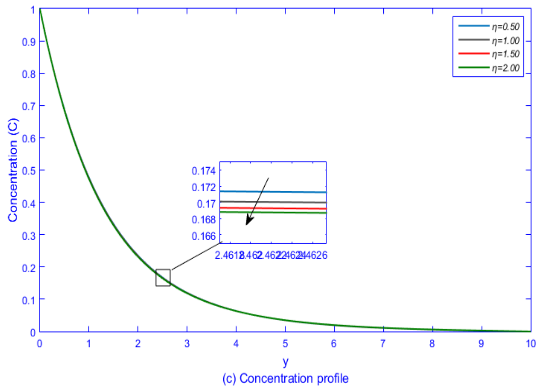

[Fig.4: Effect of Different values of Casson Fluid Parameter]

The impact of the Casson fluid parameter is seen in Figure 6. The function of the viscous force in fluid movement inside the Casson fluid is evidently of great significance. As seen in Figure 9-a, it can be observed that the magnitude of the viscous force diminishes as the Casson fluid parameter approaches infinity. Consequently, this reduction in the viscous force results in an augmentation of the fluid velocity. The observed rise leads to a quick reduction in the thermal boundary layer and the subsequent induction of a concentration boundary layer, as seen in Figures 9-b and 9-c, respectively.

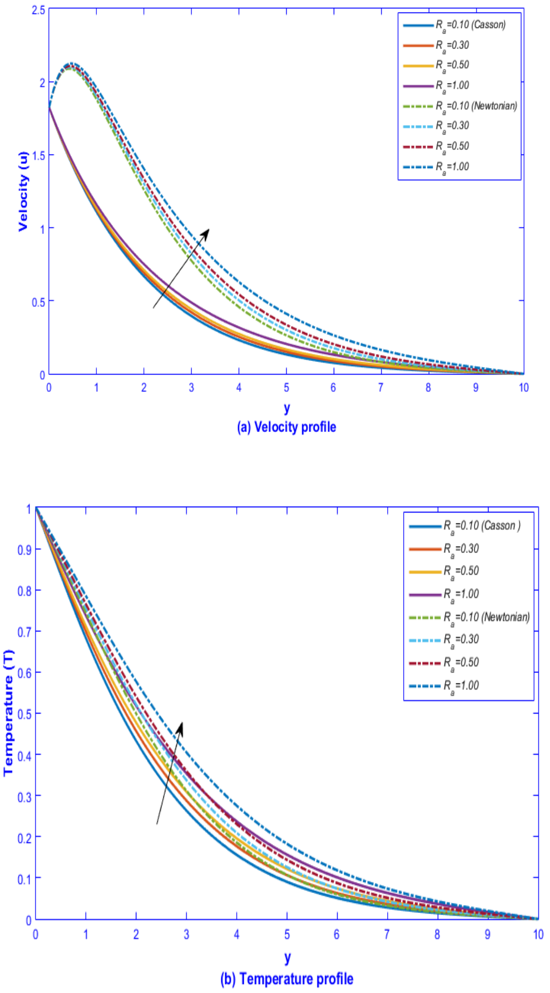

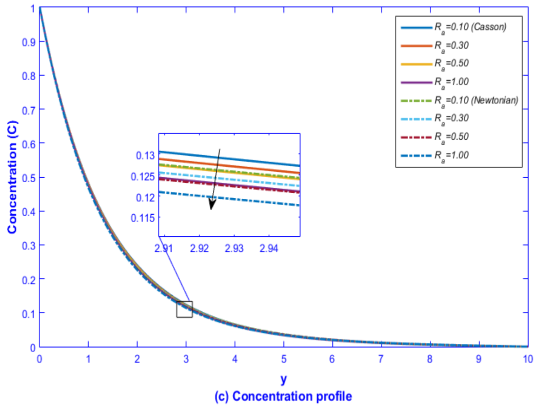

[Fig.5: Effect of Different Values of Radiation Parameter]

The impression of separate values of radiation parameter are elucidated in Figure 15. The radiation parameter is the ratio of the heat flux due to conduction to the heat flux due to radiation. This parameter is important for understanding thermal radiation heat transfer, as it helps to determine how quickly heat will be transferred from the surfaces. As increases of radiation parameter, enhance the heat transfer. An increase in the radiation parameter signifies a greater contribution of radiation to overall heat transfer, which accelerates heat dissipation from the surfaces. As a consequence, the temperature profile within the system rises, indicating an overall increase in temperature (see on the Figure 15-b). Higher temperatures have a noteworthy impact on the fluid's properties, including

Table.I: Local shear stress, Nusselt number, Sherwood number for different parameters

													Casson fluid			Newtonian fluid		
M	η	K	S_c	E_c	G_m	G_r	R_a	P_r	D_u	K_r	S_o	Q	τ	N_u	S_h	τ	N_u	S_h
3	0.5	0.6	0.6	0.02	5	10	0.5	0.71	0.5	1	0.5	0.5	2.649537	0.298397	0.750688	-1.48766	0.22825	0.76248
1													4.098438	0.267035	0.758615	-0.02577	0.2248	0.76495
5													5.364387	0.242316	0.765257	1.08701	0.22373	0.76687
7													6.493433	0.221708	0.77103	1.99346	0.22222	0.76865
	1												0.418165	0.286705	0.752101	-1.48766	0.22825	0.76248
	1.5												-0.274388	0.275936	0.75391	-1.48766	0.22825	0.76248
	2												-0.604342	0.268193	0.755266	-1.48766	0.22825	0.76248
		0.2											8.066253	0.296841	0.754454	0.62221	0.3021	0.74971
		0.4											3.792467	0.302297	0.75058	-1.0496	0.25005	0.75874
		0.8											0.570255	0.281509	0.752727	-2.26608	0.17756	0.77098
			0.7										2.760555	0.251058	0.986299	-1.39923	0.18686	1.00137
			0.9										2.855825	0.197307	1.241221	-1.32296	0.13732	1.25896
			1										2.928148	0.14582	1.478593	-1.2646	0.08859	1.49808
				0.04									2.520972	0.216519	0.767915	-1.76476	0.01788	0.79979
				0.06									2.381054	0.131201	0.785378	-2.32853	-0.38546	0.86065
				0.08									2.226149	0.041129	0.803206	-5.40157	-2.76409	1.09572
					1								4.237372	0.302837	0.750646	-0.13702	0.27433	0.75401
					3								3.443908	0.301213	0.750528	-0.81132	0.25318	0.75785
					10								0.660674	0.286112	0.752313	-3.18498	0.14913	0.77755
						3							5.954773	0.302139	0.752225	1.26009	0.31693	0.7474
						5							5.018534	0.303813	0.751205	0.50041	0.30147	0.7499
						15							0.206611	0.277345	0.753371	-3.78581	0.05979	0.79055
							0.1						2.73617	0.329108	0.747222	-1.44657	0.24768	0.76159
							0.3						2.689184	0.312407	0.749142	-1.46881	0.23723	0.76208
							1						2.571922	0.271208	0.75352	-1.52478	0.21038	0.76326
								1					2.749373	0.333817	0.746666	-1.44035	0.25059	0.76146
								2					2.950592	0.405963	0.737387	-1.34639	0.29229	0.75951
								3					3.071421	0.448266	0.731433	-1.29017	0.31449	0.75858
									0.1				2.797842	0.386315	0.732628	-1.37129	0.32776	0.74248
									1				2.452368	0.178597	0.775699	-1.64546	0.09114	0.7904
									1.5				2.240182	0.045716	0.803964	-1.81935	-0.06296	0.82223
										0.1			2.255241	0.387717	0.211536	-1.78721	0.28512	0.23563
										0.5			2.497912	0.342115	0.509598	-1.60328	0.26063	0.52585
										1.5			2.742834	0.262518	0.933287	-1.41615	0.19844	0.94265
											0.01		2.667684	0.29638	0.766851	-1.4797	0.2295	0.76708
											0.1		2.664394	0.296743	0.763931	-1.48117	0.22929	0.76619
											1		2.630396	0.300574	0.733488	-1.49567	0.22681	0.75846
												1	3.069482	0.528445	0.706146	-1.15458	0.4944	0.71241
												1.5	3.336416	0.699448	0.668041	-0.95253	0.67978	0.67273
												2	3.532384	0.840792	0.635144	-0.80604	0.82901	0.6386

viscosity. With increasing temperature, viscosity tends to decrease, leading to a less viscous fluid. In fluid dynamics, this reduction in viscosity promotes a corresponding increase in fluid velocity. The lower viscosity facilitates easier flow and less resistance within the fluid, thus contributing to enhanced fluid motion which is illustrated in Figure 15-a. The concentration profile depicted in Figure 15-c exhibits a decreasing effect with incline the radiation parameter. The responsive behavior of the local shear stress, Nusselt and sherwood number versus the dimensionless time t with all of the problem related parameters has been tabulated and can be found in Table 1. It's interesting to note that as the magnetic parameter (M), schimdt number (S_c), and chemical reaction parameter (K_r) are applied more and

Published By:
Blue Eyes Intelligence Engineering
and Sciences Publication (BEIESP)

more, the local shear stress (τ) and sherwood number (S_h) goes rises, and nusselt number (N_u) goes down. But, a transverse effect is notable for prandtl number (P_r) and heat absorption parameter in the sector of sherwood number (S_h) and nusselt number (N_u). When, the magnetic parameter (M) grows, it enhances the impact of the magnetic field on the fluid flow. The intensified magnetic field gives rise to enhanced resistance to fluid motion, hence causing a rise in the magnitude of local shear stress (τ). Concurrently, the magnetic field has the capability to hinder convective heat transmission, resulting in a reduction in the Nusselt number (N_u), due to a decrease in heat transfer efficiency. Nevertheless, the impact on mass transfer leads to an increase in the Sherwood number (S_h) as a result of enhanced solute or particle transportation. A similar pattern is seen when looking at other parameters that do not include the casson fluid parameter (η). This decreases the local shear stress (τ) and the nusselt number (N_u), but it increases the sherwood number (S_h). The porous permeability parameter (K) and Soret number (S_o) exhibit a positive correlation with the inclined Nusselt number (N_u), indicating that an increase in (K) and (S_o) leads to a rise in (N_u). Conversely, the local shear stress (τ) and Sherwood number (S_h) display a negative correlation with the aforementioned parameters, suggesting that an increase in (K) and (S_o) results in a drop in local shear stress (τ) and sherwood number (S_h). It is worth noting that based on the data presented in Table 1, the Dufour number (D_u), radiation number (R_a), thermal Grashof number (G_r), solutal Grashof number (G_m), Eckert number (E_c), and Casson fluid parameter (η) exhibit a decreasing effect on the local shear stress (τ) and an opposite trend in the case of the Sherwood number (S_h).

VII. COMPARISON

Table II: Comparison of the Present Study with Several Published Studies for Casson Fluid

Effect on \ output	Present result	Published results: Sandeep et al. [26]	K. K. Asogwa [27][28][29][30]	M. Das et al. [1]
Magnetic parameter				
u	Dec.	Dec.	Dec.	Dec.
T	Inc.	Inc.	Inc.	Inc.
C	Dec. then Inc.	Inc.	-	Inc.
τ	Inc.	Dec.	Inc.	Inc.
N_u	Dec.	Dec.	Inc.	Dec.
S_h	Inc.	Dec.	Inc.	Dec.

The subsequent Table 2 presents a qualitative comparison between the present study and several previously published studies. The main focus of the present study is to investigate the flow regime of the unsteady MHD Casson fluid past a vertical flat plate in the presence of a porous medium, whereas Sandeep et al. (2015) [26] conducted an analysis on the heat and mass transmission properties of a stretched magnetohydrodynamic surface using a similar Casson fluid across an exponentially permeable. The impacts of heat and mass transport were taken into account as Asogwa, K. K., et al. (2020) [27] investigated the magnetohydrodynamic (MHD) Casson fluid flow via a permeable stretched sheet. And, the hydromagnetic heat and mass transfer flow of a Casson fluid across an unstable stretched surface with convective boundary condition was studied by M. Das et al [1]. in 2017.

VIII. CONCLUSION

In this investigation, heat and mass transfer influences on Casson fluid flow past a semi-infinite vertical flat plate with thermal and solutal boundary layer condition have been studied. This study centers its attention on the phenomena of fluid flow and heat transfer, using governing equations as a means to describe and analyze these processes. The equations are converted into a dimensionless form in order to facilitate analysis. Dimensionless parameters play a crucial role in characterizing fluid flow and heat transfer phenomena by being recognized within the governing equations. The research employs an explicit finite difference technique to solve the modified equations and ascertain characteristics such as velocity, temperature, and concentration profiles. The results indicate that the aforementioned qualities exhibit variations in relation to dimensionless factors, hence offering valuable insights into their impact on the features of fluid flow and heat transfer. The study's most notable results are succinctly outlined as follows.

- Numerical finite difference methods have been employed for discretization with a grid size of $m = 400$, where the steady-state is evaluated at time $t = 6.0$.
- The problem exhibits convergence at $P_r \geq 0.21$, $0.21 \leq S_c \geq 15$, $K_r \leq 20$ and $\eta \geq 0.2$.
- Fluid velocity rises with the rises in radiation parameter, Eckert number and Prandtl number, whereas it decreases with the increasing value of Casson fluid parameter and magnetic number.
- The temperature of Casson fluid increases with induces of magnetic parameter and all other parameter are represents the opposite manner.
- The concentration of solutes or particles within the fluid decreases near the plate and increases far away from the plate as the magnetic parameter increases.
- The local shear stress profile represents the incline effect for magnetic parameter (M), schimdt number (S_c),

Radiation parameter (R_a) and chemical reaction parameter (K_r).

- Sherwood number shows a decrement issue against magnetic parameter (M) and radiation parameter (R_a).
- Nusselt number displays an escalating nature with gowing values of magnetic parameter (M), Casson fluid parameter (η) and Radiation parameter (R_a).

DECLARATION STATEMENT

After aggregating input from all authors, I must verify the accuracy of the following information as the article's author.

- **Conflicts of Interest/ Competing Interests:** Based on my understanding, this article has no conflicts of interest.
- **Funding Support:** This article has not been sponsored or funded by any organization or agency. The independence of this research is a crucial factor in affirming its impartiality, as it has been conducted without any external sway.
- **Ethical Approval and Consent to Participate:** The data provided in this article is exempt from the requirement for ethical approval or participant consent.
- **Data Access Statement and Material Availability:** The adequate resources of this article are publicly accessible.
- **Authors Contributions:** The authorship of this article is contributed equally to all participating individuals.

REFERENCES

1. M. Das, R. Mahato, R. Nandkeolyar, Newtonian heating effect on unsteady hydromagnetic Casson fluid flow past a flat plate with heat and mass transfer, Alexandria Engineering Journal, Volume 54, Issue 4, 2015, Pages 871-879, ISSN 1110-0168, doi: https://doi.org/10.1016/j.aej.2015.07.007.
2. A. Mahdy, Soret and Dufour effect on double diffusion mixed convection from a vertical surface in a porous medium saturated with a non-Newtonian fluid, Journal of Non-Newtonian Fluid Mechanics, Volume 165, Issues 11–12, 2010, Pages 568-575, ISSN 0377-0257. doi: https://doi.org/10.1016/j.jnnfm.2010.02.013.
3. R.K. Dash, K.N. Mehta, G. Jayaraman, Casson fluid flow in a pipe filled with a homogeneous porous medium, International Journal of Engineering Science, Volume 34, Issue 10, 1996, Pages 1145-1156, ISSN 0020-7225, doi: https://doi.org/10.1016/0020-7225(96)00012-2.
4. Shankar Goud Bejawada, Yanala Dharmendar Reddy, Wasim Jamshed, Kottakkaran Sooppy Nisar, Abdulaziz N. Alharbi, Ridha Chouikh, Radiation effect on MHD Casson fluid flow over an inclined non-linear surface with chemical reaction in a Forchheimer porous medium, Alexandria Engineering Journal, Volume 61, Issue 10, 2022, Pages 8207-8220, ISSN 1110-0168, doi: https://doi.org/10.1016/j.aej.2022.01.043.
5. A. Mahdy, Soret and Dufour effect on double diffusion mixed convection from a vertical surface in a porous medium saturated with a non-Newtonian fluid, Journal of Non-Newtonian Fluid Mechanics, Volume 165, Issues 11–12, 2010, Pages 568-575, ISSN 0377-0257, doi: https://doi.org/10.1016/j.jnnfm.2010.02.013
6. Shahzad, H., Wang, X., Ghaffari, A. *et al.* Fluid structure interaction study of non-Newtonian Casson fluid in a bifurcated channel having stenosis with elastic walls. Sci Rep **12**, 12219 (2022). doi: https://doi.org/10.1038/s41598-022-16213-3.
7. R. Srinivasa Raju, B. Mahesh Reddy & G. Jithender Reddy (2017) Finite element solutions of free convective Casson fluid flow past a vertically inclined plate submitted in magnetic field in presence of heat and mass transfer, International Journal for Computational Methods in Engineering Science and Mechanics, 18:4-5, 250-265, doi: https://doi.org/10.1080/15502287.2017.1339139
8. Fung, Y. C., and Skalak, R. (November 1, 1981). "Biomechanics: Mechanical Properties of Living Tissues." ASME. J Biomech Eng. November 1981; 103(4): 231–298. doi: https://doi.org/10.1115/1.3138285.
9. Mustafa, M., Hayat, T., Pop, I. and Aziz, A. (2011) Unsteady Boundary Layer Flow of a Casson Fluid Due to an Impulsively Started Moving Flat Plate. Heat Transfer-Asian Research, 40, 563-576. http://dx.doi.org/10.1002/htj.20358
10. Khan H, Ali F, Khan N, Khan I and Mohamed A (2022) Electromagnetic flow of Casson nanofluid over a vertical Riga plate with ramped wall conditions. *Front.Phys.* 10:1005447. doi: https://doi.org/10.3389/fphy.2022.1005447.
11. Prameela, M., Gangadhar, K., & Reddy, G. J. (2022, June 1). MHD free convective non-Newtonian Casson fluid flow over an oscillating vertical plate. doi: https://doi.org/10.1016/j.padiff.2022.100366
12. Asma Khalid, Ilyas Khan, Arshad Khan, Sharidan Shafie, Unsteady MHD free convection flow of Casson fluid past over an oscillating vertical plate embedded in a porous medium, Engineering Science and Technology, an International Journal, Volume 18, Issue 3, 2015, Pages 309-317, ISSN 2215-0986, doi: https://doi.org/10.1016/j.jestch.2014.12.006.
13. Benazir, A. J., Sivaraj, R., & Makinde, O. D. (2015, December 1). Unsteady Magnetohydrodynamic Casson Fluid Flow over a Vertical Cone and Flat Plate with Non-Uniform Heat Source/Sink. doi: https://doi.org/10.4028/www.scientific.net/jera.21.69
14. Goud, B. S., Kumar, P. P., & Malga, B. S. (2020, December 1). Effect of Heat source on an unsteady MHD free convection flow of Casson fluid past a vertical oscillating plate in porous medium using finite element analysis. doi: https://doi.org/10.1016/j.padiff.2020.100015.
15. Sulochana, C., Poornima, M. Unsteady MHD Casson fluid flow through vertical plate in the presence of Hall current. SN Appl. Sci. 1, 1626 (2019). doi: https://doi.org/10.1007/s42452-019-1656-0.
16. Oyekunle, T. L., & Agunbiade, S. A. (2020, December 1). Diffusion-thermo and thermal-diffusion effects with inclined magnetic field on unsteady MHD slip flow over a permeable vertical plate. doi: https://doi.org/10.1186/s42787-020-00110-7.
17. B. Narsimha Reddy, P. Maddileti and B. Shashidar Reddy, Nanofluid flow on non-linearly stretching surface influenced by the combined effects of Soret and Dufour with chemical reaction, JP Journal of Heat and Mass Transfer 30 (2022), 161-182. doi: http://dx.doi.org/10.17654/0973576322062.
18. Hayat, T., Yasmin, H., & Al-Yami, M. (2014, January 1). Soret and Dufour effects in peristaltic transport of physiological fluids with chemical reaction: A mathematical analysis. doi: https://doi.org/10.1016/j.compfluid.2013.10.038
19. Krishnamurthy, M. R., Gireesha, B. J., Prasannakumara, B. C., & Gorla, R. S. R. (2016, January 1). Thermal radiation and chemical reaction effects on boundary layer slip flow and melting heat transfer of nanofluid induced by a nonlinear stretching sheet. doi: https://doi.org/10.1515/nleng-2016-0013.
20. Mukhopadhyay, S., & Layek, G. C. (2008, May 1). Effects of thermal radiation and variable fluid viscosity on free convective flow and heat transfer past a porous stretching surface. doi: https://doi.org/10.1016/j.ijheatmasstransfer.2007.11.038.
21. Kumar, K. A., Sugunamma, V., & Sandeep, N. (2019, November 8). Effect of thermal radiation on MHD Casson fluid flow over an exponentially stretching curved sheet. doi: https://doi.org/10.1007/s10973-019-08977-0.
22. Mahato, R., Das, M. Effect of suction/blowing on heat-absorbing unsteady radiative Casson fluid past a semi-infinite flat plate with conjugate heating and inclined magnetic field. Pramana - J Phys 94, 127 (2020). doi: https://doi.org/10.1007/s12043-020-01990-1.
23. Amanulla, C., Nagendra, N., & Reddy, M. S. (2018, March 26). Computational analysis of non-Newtonian boundary layer flow of nanofluid past a semi-infinite vertical plate with partial slip doi: https://doi.org/10.1515/nleng-2017-0055.
24. Rao, S. N., Vidyasagar, G., & Deekshitulu, G. V. S. R. (2021, January 1). Unsteady MHD free convection Casson fluid flow past an exponentially accelerated infinite vertical porous plate through porous medium in the presence of radiation absorption with heat generation/absorption. doi: https://doi.org/10.1016/j.matpr.2020.07.554.
25. Raju, C. S. K., Sandeep, N., Sugunamma, V., Babu, M. R., & Reddy, J. V. R. (2016, March 1). Heat and mass transfer in magnetohydrodynamic Casson fluid over an exponentially permeable stretching surface. doi: https://doi.org/10.1016/j.jestch.2015.05.010.
26. Asogwa, K. K., & Ibe, A. A. (2020, August 24). A Study of MHD Casson Fluid Flow over a Permeable Stretching Sheet with Heat and Mass Transfer. doi:

https://doi.org/10.9734/jerr/2020/v16i217161.

27. Sarma, S., & Ahmed, N. (2022, August 3). Dufour effect on unsteady MHD flow past a vertical plate embedded in porous medium with ramped temperature. doi: https://doi.org/10.1038/s41598-022-15603-x.
28. Shekar P, R., Narla V. K., P. K. M., & R, B. (2020). Thermal Radiation Effect on Entropy in Hydromagnetic Peristaltic Flow of a Jeffrey Nanofluid Through an Unsymmetrical Channel. In International Journal of Innovative Technology and Exploring Engineering (Vol. 9, Issue 6, pp. 2015–2021). doi: https://doi.org/10.35940/ijitee.d2046.049620
29. Rao B, V., Konda, Jayaramireddy, & Ganteda, C. (2019). MHD And Thermal Radiation Effects of a Nanofluid over a Stretching Sheet Using HAM. In International Journal of Recent Technology and Engineering (IJRTE) (Vol. 8, Issue 4, pp. 3489–3496). doi: https://doi.org/10.35940/ijrte.c6726.118419
30. Hemalatha, S. V., & Ratchagar, N. P. (2019). Modeling the Transport of Hydrocarbons in the Subsurface Environment with Chemical Reaction. In International Journal of Engineering and Advanced Technology (Vol. 9, Issue 1s4, pp. 970–973). doi: https://doi.org/10.35940/ijeat.a1205.1291s419

AUTHORS PROFILE

Riaz Hossain received the B.Sc. Degree in Mathematics from Bangabandhu Sheikh Mujibur Rahman Science and Technology University, Gopalganj-8100, Dhaka, Bangladesh. Now I am currently pursuing an M.Sc. degree in Applied Mathematics from the same University. I am interested in research fields including Aerodynamics, Fluid Mechanics, Thermodynamics, Production and Industrial Engineering.

Dr. Muhammad Minarul Islam presently working as an Associate Professor with the Department of Mathematics at Bangabandhu Sheikh Mujibur Rahman Science and Technology University, Gopalganj-8100, Dhaka, Bangladesh. He received PhD degree in Mechanical Engineering from the university of Kitakyushu, Japan. He has authored more than 25 papers in international journal. His research interested including Fluid Mechanics, Gas Dynamics and Computational Fluid Dynamics.